

Effects of Biceps Tension and Superior Humeral Head Translation on the Glenoid Labrum

Eunjoo Hwang,^{1,2} James E. Carpenter,³ Richard E. Hughes,^{2,3,4} Mark L. Palmer^{1,2,5}

¹School of Kinesiology, University of Michigan, Ann Arbor, Michigan, ²Department of Biomedical Engineering, University of Michigan, Ann Arbor, Michigan, ³Department of Orthopaedic Surgery, University of Michigan, Ann Arbor, Michigan, ⁴Department of Industrial and Operations Engineering, University of Michigan, Ann Arbor, Michigan, ⁵Reveal Technologies Group, Grand Rapids, Michigan

Received 29 October 2013; accepted 17 June 2014

Published online 28 July 2014 in Wiley Online Library (wileyonlinelibrary.com). DOI 10.1002/jor.22688

ABSTRACT: We sought to understand the effects of superior humeral head translation and load of the long head of biceps on the pathomechanics of the superior glenoid labrum by predicting labral strain. Using micro-CT cadaver images, a finite element model of the glenohumeral joint was generated, consisting of humerus, glenoid bone, cartilages, labrum, and biceps tendon. A glenohumeral compression of 50 N and biceps tensions of 0, 22, 55, and 88 N were applied. The humeral head was superiorly translated from 0 to 5 mm in 1-mm increments. The highest labral strain occurred at the interface with the glenoid cartilage and bone beneath the origin of the biceps tendon. The maximum strain was lower than the reported failure strain. The humeral head motion had relatively greater effect than biceps tension on the increasing labral strain. This supports the mechanistic hypothesis that superior labral lesions result mainly from superior migration of the humeral head, but also from biceps tension. © 2014 Orthopaedic Research Society. Published by Wiley Periodicals, Inc. *J Orthop Res* 32:1424–1429, 2014.

Keywords: biceps; FE; labrum; rotator cuff; shoulder

Pathologic changes of the superior shoulder labrum are common, yet poorly understood. The most common pathology is a fraying or partial tearing of the labrum, coined a type-I SLAP (superior labral anterior–posterior) tear by Snyder et al. in 1995.¹ However, detachment of the labrum from the superior glenoid bone, classified as a type-II tear, is considered the most common symptomatic injury. These tears occur most commonly in the region of the labrum where the biceps tendon attaches to the labrum and superior glenoid. They can extend more posterior or anterior or both anterior and posterior from that location as they increase in length along the glenoid rim.² These injuries are thought to occur from sudden, excessive loads or from repetitive microtrauma to the labrum as a result of loading from the long head of the biceps tendon or from superior translation of the humeral head. Tears in the superior labrum are most common in association with rotator cuff tears, where they may be secondary to pathologic joint loading that occurs as a result of the loss of rotator cuff function.² They can also occur in athletes or laborers who experience high loads across the joint and in the biceps tendon.

Understanding the factors leading to labral tears would better inform current treatments, which include repair, partial removal, or biceps tendon detachment. However, the pathomechanics of these tears and the relationship to humeral head translation and loading of the biceps tendon are unclear. It has been impossible to adequately study the interaction of these factors in vivo or in a cadaveric model, due to the inability to experimentally measure stress and strain in the

interior of the labrum tissue. A finite element (FE) model allows for estimation of stresses and strains below the surface of the tissue, which is required to understand the risk of mid-substance failure. We report on the further development and implementation of an FE model of the superior labrum.

We sought to understand the effect of the superior translation of the humeral head relative to the glenoid cavity (as can be seen in cases of rotator cuff tears) combined with tensile loading on the long head of the biceps tendon on the superior labrum. We hypothesized that: (1) the regions of highest strains in the labrum occur along a crescent in the mid-substance of the superior labrum corresponding to common superior labral lesions (type II); (2) increasing load on the long head of the biceps tendon causes increased strain in the labrum; and (3) the effect of humeral head translation on the increasing strain in the labrum is greater than the effect of biceps tension. These hypotheses were tested using the FE model validated by comparison with mechanical testing of cadaveric specimens.³

METHODS

Development of a Finite Element Model

The geometries of the glenoid, humeral head, labrum, long head of the biceps tendon, and articular cartilage were acquired from a fresh frozen cadaveric shoulder (male, 84 years old) by sequential imaging using the GE eXplore Locus (GE Healthcare, London, Canada) micro-CT system at a voxel size of 93 μm followed by a Boolean operation.³ The images were reconstructed at a resolution of 186 μm using a cone-beam back-projection algorithm. Segmentation was performed using commercial software (Amira 5.3, Visage Imaging, Inc., San Diego, CA).

The FE mesh was generated using a preprocessing tool (Hypermesh 10, Altair Engineering, Inc., Troy, MI) with validated threshold settings.³ The bones were modeled using shell elements. The cartilages, labrum, and biceps tendon were converted to hexahedral elements. Solid elements were

Conflict of interest: None.

Grant sponsor: Valassis Endowed Research Fund; Grant sponsor: University of Michigan, Department of Orthopaedic Surgery.

Correspondence to: Mark L. Palmer (T: 734-647-7645;

F: 734-936-1925; E-mail: mlpalmer@umich.edu)

© 2014 Orthopaedic Research Society. Published by Wiley Periodicals, Inc.

added to the distal end of the biceps tendon to extend the tendon from the site of attachment on the labrum over the humeral head and through the bicipital groove (Fig. 1). Appropriate mesh densities were determined by convergence studies.³ The labrum was modeled as transversely isotropic, hyperelastic material^{4,5} with four elastic moduli (21.3, 15.4, 19.3, and 20.9 MPa for superior, anterior, inferior, and posterior labrum, respectively).^{3,5} The biceps tendon was modeled as an isotropic, hyperelastic material with an elastic modulus of 629 MPa.⁶ Cartilage was modeled as isotropic elastic (0.66 and 1.7 MPa for humerus and glenoid, respectively),^{7,8} and bones were modeled as rigid materials.

Loading Conditions

The humerus and glenoid had their own local coordinate systems. The center of the head was assigned as the origin of the humerus coordinate system. For the humerus, the local Z-axis was parallel to the humeral shaft and directed inferiorly. The local Y-axis was perpendicular to the Y-axis and pointed laterally. The local X-axis was defined by the common line perpendicular to the Z and Y axes and directed anteriorly. Similarly, the origin of the glenoid coordinate system was placed at the midpoints of the long and short axes of the glenoid. The local Y-axis for the glenoid was parallel to the posterior and anterior glenoid axis, pointing superiorly. The X-axis was perpendicular to the Y-axis, and directed anteriorly. The local Z-axis for the glenoid was defined by the cross-product of the other two axes and pointed laterally.

The humeral head was positioned in 30° of glenohumeral abduction in the scapular plane without humeral rotation.³ The glenoid was constrained in all 6° of freedom. A 50-N compressive load was applied to seat the humerus in the glenoid cavity.^{3,9} The humerus was superiorly translated up to

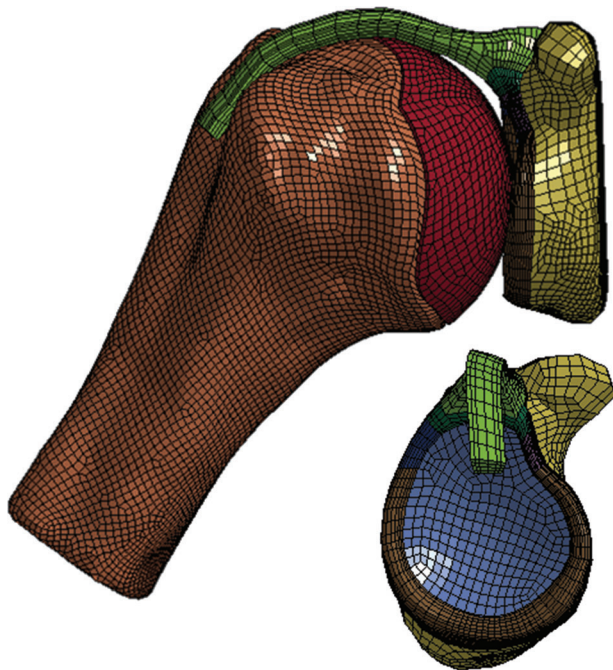


Figure 1. A 3D hexahedral FE model of the glenohumeral joint, including the long head of biceps tendon. The humerus was positioned in 30° of abduction in the scapular plane with centric humeral rotation. The humerus is shown in coronal view and is hidden in lateral view.

5 mm in 1-mm increments.³ This amount of head displacement was chosen to encompass the range of displacements encountered clinically in patients with massive rotator cuff disease.¹⁰

We tested four conditions for the biceps tension: 0, 22, 55, and 88 N. A 22-N load was chosen because it affects the glenohumeral range of motion and kinematics.³ A 55-N load was used because it represents the force of maximum isometric contraction calculated from physiologic cross-sectional area of the long head of the biceps muscle.¹¹ We also tested 88 N of tensile loading¹² to evaluate the effects of increased force generation during stretch of an activated muscle, or an eccentric contraction, when whole muscles are capable of resisting up to 160% of the maximum isometric force.¹³ The force vector paralleled the line connecting the midpoint of the greater and lesser tuberosities of the humerus to the midpoint of the crest of the greater and lesser tuberosities of the humerus.

Dynamic Analyses and Statistics

Analyses were performed using LS-DYNA (Livermore Software Tech. Corp., Livermore, CA). All sliding interfaces were modeled using frictionless, surface-to-surface contact due to the low coefficient of friction in synovial joints.^{3,14} The von Mises strain was predicted from the FE model, because it is a scalar quantity representing the combined effect of all components of the material strain tensor and indicative of the energy required to distort the material. The strain for a cross section through the labrum was calculated by performing a volume-weighted average of the strains for the elements within that area.

RESULTS

FE Predictions of Strain in the Labrum

The highest strain in the superior labrum occurred at the interface with the glenoid cartilage and glenoid bone (Fig. 2D). The high-strain region extended both along an arc from about -20° to +40° (Fig. 2E) and radially through the labrum from the bone-cartilage interface surface to the free surface (Fig. 2D, inset). This strain pattern corresponds well with an arthroscopic image of a type-II SLAP lesion (Fig. 2F).

Effect of Biceps Tension on Labrum Strain

When the load on the biceps was increased, strain in the superior labrum increased (Figs. 2 and 3). The high-strain region extended from the origin of the biceps on the superior surface of the labrum to the glenoid bone and cartilage interface on the inferior surface of the labrum (Fig. 2C,D, insets). Increasing the biceps load caused an increase in the strain magnitude in the circumferential direction and involved more of the superior labrum from -40° to +40° (Fig. 2C,D). The highest strain was located at 0°. Increasing the biceps tension from 0 to 88 N increased the strain by a factor of 27% at 0 mm and 40% at 5 mm of humeral head displacement (Fig. 3). The region of the labrum with the highest strain was independent of the magnitude of the biceps load (Fig. 3).

Effect of Superior Humeral Head Translation

Increasing the translation of the head in the superior direction caused an increase in the strain in the

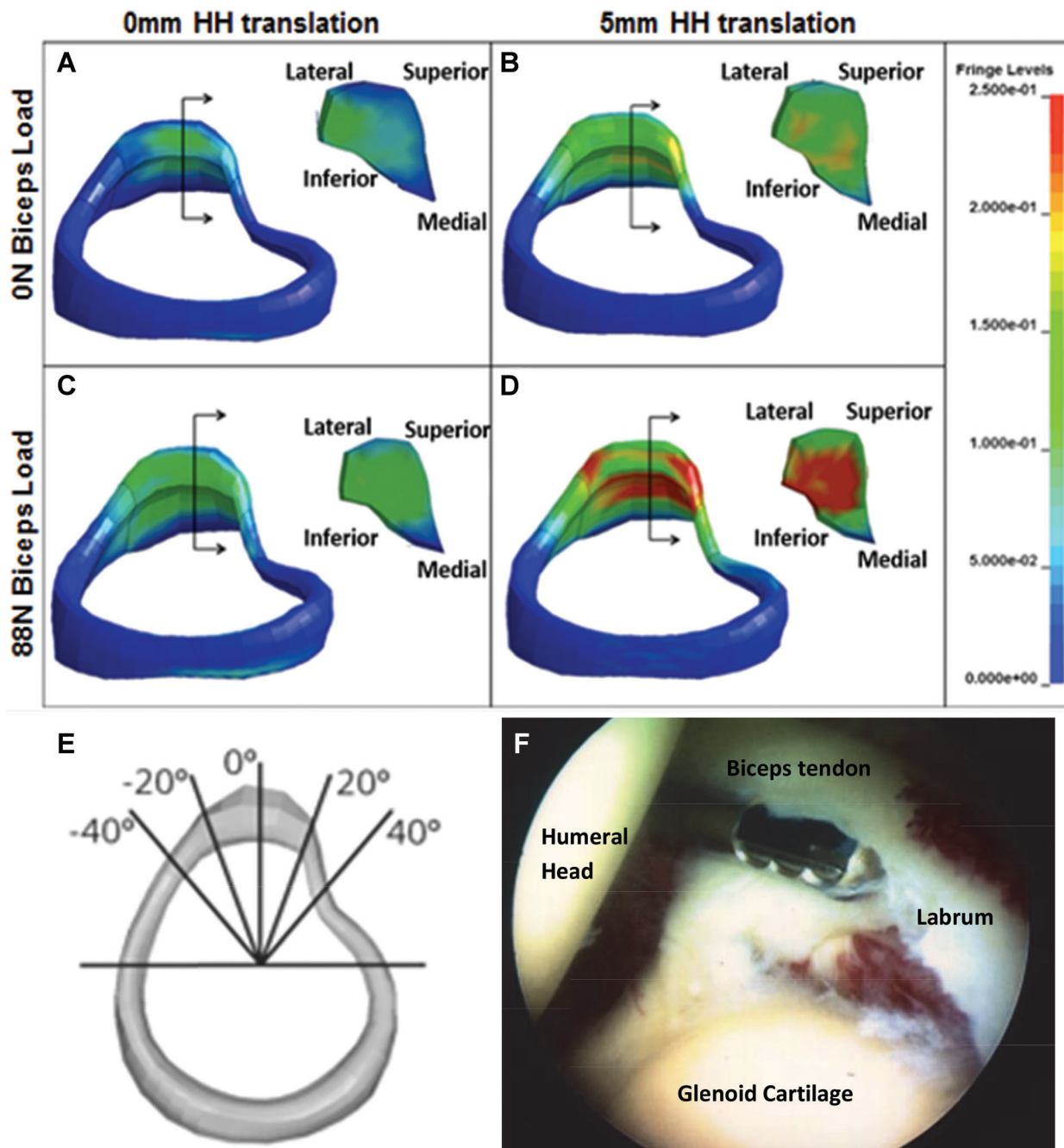


Figure 2. Strain distribution after application of a 50 N compressive load on the humeral head with the following conditions of superior head translation and biceps load: (A) 0 mm, 0 N; (B) 5 mm, 0 N; (C) 0 mm, 88 N; and (D) 5 mm, 88 N. A lateral view of the strain distribution over the glenoid labrum is shown from a slightly inferior perspective. The inset represents the strain distribution across a section through the labrum expressed by the vertical black line with two arrow heads. The strain magnitude is shown by the scale at right. (E) The specific locations along the superior labrum. (F) An arthroscopic image of a type-II SLAP lesion.

superior labrum (Figs. 3 and 4). We observed the strain at 0°, coincident with the area of the highest strain (Fig. 4). Translation of the head from 0 to 5 mm resulted in an increase in strain >100% for each magnitude of long head of biceps load.

DISCUSSION

We sought to understand the behavior of the superior labrum in the presence of a rotator cuff tear and

loading of the long head of the biceps tendon using the strain pattern predicted by an FE model. The highest strains in the labrum were found along a crescent in the mid-substance of the superior labrum in the area between -20° and 20° where these tears are most commonly seen clinically (Fig. 2) and in other published images for a type-II SLAP lesion.^{1,3,15} Increasing the load on the biceps tendon increased the strain in the labrum (Figs. 3 and 4). The effect of humeral

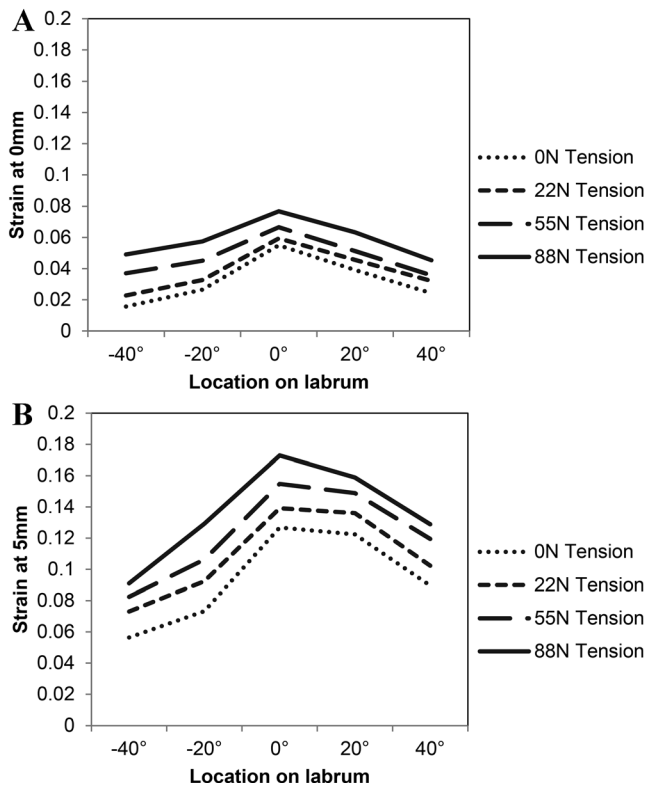


Figure 3. Strain in the labrum due to biceps tendon at (A) 0mm and (B) 5mm of humeral head translation. Increasing biceps tension caused an increase in overall labral strain.

head translation on increasing the labral strain is greater than the effect of the biceps tendon. Therefore, our results support the mechanistic hypothesis that a SLAP lesion may occur as a result of superior migration of the humeral head regardless of the amount of biceps load.

The current study supports experimental evidence that an unstable shoulder increases the susceptibility of the labrum to injury. To generate the conditions for an unstable shoulder, Rizio et al.¹⁶ generated a Bankart lesion, an avulsion of the anteroinferior glenoid labrum, and then sutured the damaged tissue. They

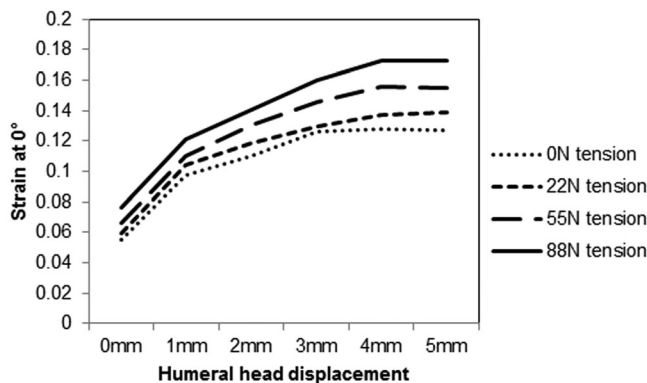


Figure 4. Strain in labrum due to humeral head translation. Increasing head migration caused an increase in strain at the superior labrum underneath the biceps tendon attachment.

found that increased instability caused greater labral strain. Similarly, our study showed that the strain in the superior labrum increased with increasing superior migration of the humeral head (Figs. 3 and 4). In the current model, a compressive force between the head and the glenoid cavity combined with superior translation of the head causes compression and shear of the superior labrum at the interface with the glenoid cartilage and glenoid bone. The load directed medially by the humeral head combined with tension from the biceps tendon directed superiorly results in a plane of high strain at the origin of the biceps tendon on the glenoid bone (Fig. 2).

The FE model predicts that the tension of the biceps tendon is transferred and dissipated by the labrum along pathways in the radial and circumferential direction. First, at 50 N of compressive force between the humeral head and glenoid and no biceps load prior to superior translation of the head, the strain field in the cross section of the labrum is relatively low (Fig. 2A, inset). When the load on the biceps is increased under these conditions, strain also increases in the cross section of the labrum (Fig. 2C, inset). Therefore the predicted strain field demonstrates a loading pathway from the attachment of the biceps on the superior labrum to the glenoid bone and cartilage interface on the inferior labrum (Fig. 2C, inset). Similarly, comparing 0 N of biceps load at 5 mm of humeral head translation (Fig. 2B, inset) with 88 N of load at 5 mm of translation (Fig. 2D, inset), a high-strain pathway exists from the origin of the biceps tendon on the superior surface of the labrum to the interface of the inferior surface of the labrum with the glenoid bone and cartilage. Second, the biceps force is also transferred from the biceps attachment site circumferentially through the labrum in both anterior and posterior directions. At 0 N of biceps load and 50 N of compressive force (Fig. 2A,B), the model predicted low strain levels in the circumferential direction from -20° to $+20^{\circ}$. Increasing the biceps load causes an increase in the strain magnitude in the circumferential direction and involves more of the superior labrum from -40° to $+40^{\circ}$ (Fig. 2C,D).

The higher strain on the anterior side compared to the posterior side (Fig. 3) can be explained by the anatomic characteristics of the specimen used to construct the model. The volume of labrum on the posterior side was larger than that on the anterior side in our specimen. The radial thickness of the anterosuperior labrum in the specimen was also smaller (3.1 mm) compared with the thickness (7.8 ± 1.3 mm) reported in the literature.⁷ Consequently, the force must pass through a smaller cross-sectional area of tissue leading to higher tissue stresses and strains. This observation suggests that the labral strain is sensitive to labrum morphology.

The strain pattern was mainly affected by the magnitude of superior humeral head translation. The shape of the strain curve as a function of humeral

head translation (Fig. 4) is determined by the size of the contact surface between the head and the labrum. At 0 mm of translation, the contact area is primarily on the glenoid cartilage and the superior labrum. With increasing translation, the contact area moves superiorly onto the superior labrum. For low biceps loads, the periphery of the labrum is relatively unconstrained so the labrum does not conform to the contour of the humeral head. Consequently, the labrum is displaced superiorly and medially in the direction of its free surface. As the load on the biceps tendon is increased, the superior labrum is pulled towards the head. For the case of 88 N of tensile load on the biceps, the load is sufficient to constrain the superior labrum to conform to the contour of the humeral head. Increased conformity between the head and the superior labrum increases the contact area between two, which in turn increases the strain in the labrum. The model also demonstrated that increasing the load on the biceps tendon from 0 to 88 N increased the total strain in the labrum by 27% at 0 mm and 40% at 5 mm of humeral head displacement (Fig. 3).

Our study has a number of limitations. The interfaces of the labrum with the connective tissues are complicated by the similarity of the composition. The properties of the superior labrum are not based on a detailed representation of the labrum microstructure, even though we used the latest published data for determining material properties.⁵ Errors in approximating the stiffness of the material would affect the strain magnitude, but not the overall strain pattern.³ The current model also assumes that the collagen fibers of the superior labrum are oriented primarily circumferentially.¹⁷ A more complex collagen fiber network particularly at the origin of the biceps tendon would reduce the strain in the mid-substance of the labrum causing higher stresses at the interface of the labrum with the superior glenoid.

Another limitation is the response of the long head of biceps muscle. The biceps tendon travels superiorly over the humeral head before attaching to the muscle. Depending on the orientation of the humeral head with respect to the glenoid, the biceps tendon may experience a stretch up to twice the displacement of the head. When skeletal muscle is activated and stretched, an eccentric contraction, the muscle force may increase by 60% compared to the isometric load.¹³ However, the long head of biceps muscle is biarticular acting across both the elbow and glenohumeral joints. The positions of both joints determine the initial length, stretch, and force of the muscle. Rather than simulate the dynamic changes in muscle force, we demonstrated the response of the labrum over a range of humeral head translations (0–5 mm) and a range of muscle forces that span 0–160% of peak isometric force in muscle. Therefore our study predicts the trends in the stress-strain state for the labrum for likely physiologic ranges of biceps loads and humeral head displacements, but does not predict a specific biceps load

or loading pathway as a function of humeral head position.

We assumed 50 N of glenohumeral compression.^{3,9} Since the effect of the biceps tension on the strain might be amplified under the low compressive force, 111 N of joint compression¹⁸ was additionally tested. A 111-N load is only 15% of body weight of a 75-kg person, but this appeared as the maximum effective compressive force to increase the joint stability.¹⁸ The simulation under this higher compressive load predicted strain distributions similar to Figure 2 and increased the strain by 2–5%. With 111 N of compression, increasing the biceps tension from 0 to 88 N increased the total strain by 27% at 0 mm and 38% at 5 mm, which was comparable to the 50-N compression condition. Similarly, the humeral head was translated up to 5 mm for massive rotator cuff tear cases. Based on clinical observations and published data,¹⁰ humeral head migration >5 mm was observed in shoulders with large ruptures of the rotator cuff, so that the strain at 5 mm of translation was reported. The strain pattern³ at 3 mm, an average amount of translation with massive rotator cuff tear,¹⁰ is similar to that at 5 mm. Thus, the assumptions about the joint compression and humeral head migration are considered to have minimal impact on the strain distribution. However, the 5 mm of head displacement superiorly may result in impingement with the acromion.

This study focused on the superior translation of the humeral head with biceps tension in one arm position to understand the mechanism of the labral tear concomitant with rotator cuff tears. However, in the future, the behavior of the labrum tissue could be investigated in multiple arm positions with various translational directions of the humeral head and diverse geometries. Labral tears are also common in young athletes, especially in overhead throwing. The late cocking¹⁶ and deceleration¹⁹ phases of pitching motion have been hypothesized to cause tears. Since both phases were simulated in external and internal humeral rotational positions with a certain amount of elevation in the scapular plane,¹⁹ this issue could be interpreted as the effect of arm position on the labral behavior. Differing arm positions could alter the primary loading vector and morphology of the biceps tendon and the compressive force in the glenohumeral joint, thus influencing the strain distribution within the labrum. For example, the externally rotated humerus shifts the vector of biceps tension posteriorly, and the anchor of the biceps tendon could be twisted off and pulled out. This could result in a greater concentration of the load at the anchor attachment and reduced compressive force in the joint. It may also increase the superior labral strain and the relative impact of the biceps tendon on the labral strain. With increased biceps tension in this specific arm position, the increased amount of labral strain would be amplified. Other translational directions of the humerus

may alter the labral strain pattern. For example, if the humeral head were translated superoposteriorly, the posterior labrum likely would register higher strain levels. If the humerus is translated posterolaterally, the biceps tendon is pulled in a more lateral direction than our testing conditions reflect. In this case, the attachment of the biceps tendon on the superior labrum could experience more stress and the biceps tension could be a more significant factor than the head translation. Similarly, the biceps tendon attachment on the superior labrum could change the primary loading vector of the biceps tendon. Thus, the area of high strain may shift depending on the anchor location of the biceps tendon.

In summary, the interactions among biceps loading, humeral translation, and labral tissue mechanics were tested with an anatomically accurate model of the glenohumeral joint. Under the conditions for this study, superior translation of the humeral head resulted in higher labral strains than did biceps tendon loading. The predicted strain pattern was consistent with tears in the superior labrum described clinically. Maximum predicted strains lower than the failure strain suggest that repetitive microtrauma or tissue fatigue rather than a single loading event may be necessary to cause a mid-substance failure of the labrum.

ACKNOWLEDGMENTS

This work was funded by an internal grant from the Valassis Endowed Research Fund and the University of Michigan, Department of Orthopaedic Surgery.

REFERENCES

1. Snyder SJ, Banas MP, Karzel RP. 1995. An analysis of 140 injuries to the superior glenoid labrum. *J Shoulder Elbow Surg* 4:243–248.
2. Morgan CD, Burkhart SS, Palmeri M, et al. 1998. Type II SLAP lesions: three subtypes and their relationships to superior instability and rotator cuff tears. *Arthroscopy* 14:553–565.
3. Hwang EJ, Carpenter J, Hughes R, et al. 2014. Shoulder labral pathomechanics with rotator cuff tears. *J Biomech* 47:1733–1738.
4. Weiss JA, Maker BN, Govindjee S. 1996. Finite element implementation of incompressible, transversely isotropic hyperelasticity. *Comput Method Appl Mech Eng* 135:107–128.
5. Smith CD, Masouros SD, Hill AM, et al. 2008. Tensile properties of the human glenoid labrum. *J Anat* 212:49–54.
6. Carpenter JE, Wening JD, Mell AG, et al. 2005. Changes in the long head of the biceps tendon in rotator cuff tear shoulders. *Clin Biomech (Bristol, Avon)* 20:162–165.
7. Carey J, Small CF, Pichora DR. 2000. In situ compressive properties of the glenoid labrum. *J Biomed Mater Res* 51:711–716.
8. Donzelli PS, Spilker RL, Ateshian GA, et al. 1999. Contact analysis of biphasic transversely isotropic cartilage layers and correlations with tissue failure. *J Biomech* 32:1037–1047.
9. Lippitt SB, Vanderhooft JE, Harris SL, et al. 1993. Glenohumeral stability from concavity-compression: A quantitative analysis. *J Shoulder Elbow Surg* 2:27–35.
10. Mura N, O'Driscoll SW, Zobitz ME, et al. 2003. The effect of infraspinatus disruption on glenohumeral torque and superior migration of the humeral head: a biomechanical study. *J Shoulder Elbow Surg* 12:179–184.
11. Su WR, Budoff JE, Luo ZP. 2010. The effect of posterolateral rotator cuff tears and biceps loading on glenohumeral translation. *Arthroscopy* 26:578–586.
12. Langenderfer J, LaScalza S, Mell A, et al. 2005. An EMG-driven model of the upper extremity and estimation of long head biceps force. *Comput Biol Med* 35:25–39.
13. McCully KK, Faulkner JA. 1985. Injury to skeletal muscle fibers of mice following lengthening contractions. *J Appl Physiol* 59:119–126.
14. Henak CR, Ellis BJ, Harris MD, et al. 2011. Role of the acetabular labrum in load support across the hip joint. *J Biomech* 44:2201–2206.
15. Nam EK, Snyder J. 2003. The diagnosis and treatment of superior labrum, anterior and posterior (SLAP) lesions. *Am J Sports Med* 31:798–810.
16. Rizio L, Garcia J, Renard R, et al. 2007. Anterior instability increases superior labral strain in the late cocking phase of throwing. *Orthopedics* 30:544–550.
17. Gatti CJ, Maratt JD, Palmer ML, et al. 2010. Development and validation of a finite element model of the superior glenoid labrum. *Ann Biomed Eng* 38:3766–3776.
18. Warner JJP, Bowen MK, Deng X, et al. 1999. Effect of joint compression on inferior stability of the glenohumeral joint. *J Shoulder Elbow Surg* 8:31–36.
19. Yeh ML, Lintner D, Luo ZP. 2005. Stress distribution in the superior labrum during throwing motion. *Am J Sports Med* 33:395–401.